EVS27
Barcelona, Spain, November 17-20, 2013

High power $LiFePO_4$ cell evaluation: fast charge, depth of discharge and fast discharge dependency

D. Anseán[1], J.C. Viera[1], M. González[1], V.M. García[2], J.C. Álvarez[1], J.L. Antuña[1]
[1]*University of Oviedo, Department of Electrical Engineering, Campus de Gijón, s/n, Módulo 3, 33204, Gijón, Asturias, Spain, anseandavid.uo@uniovi.es*
[2] *University of Oviedo, Department of Physical and Analytical Chemistry, Campus de Gijón, s/n, Edificio Polivalente, 33204, Gijón, Asturias, Spain*

Abstract

High power lithium iron phosphate (LFP) batteries suitable for Electric Vehicles are tested in this work. An extended cycle-life testing is carried out, consisting in various types of experiments: standard cycling, optimized fast charge with high constant current discharge (4 C) and simulating driving dynamic stress protocols (DST). The fast charge/DST discharge tests are carried out with depth of discharge (DOD) dependency (100% DOD and partial 50% DOD discharge). A complete analysis of the cycling results is developed, showing an overall good performance of the tested batteries. In all of experiments, long term U.S. Advanced Battery Consortium goals are met: fast charging, cycle life and specific energy. Only the long term specific energy goal is not achieved, which is a drawback intrinsic in this technology. The results provide useful information for battery selection, BMS designs and other applications in EV industry.

Keywords: Cycle life evaluation, Fast-charge protocol, Dynamic stress tests, Lithium iron phosphate

1 Introduction

Nowadays, Electric Vehicles (EVs) are experiencing a notable advance in various forms: automobile manufacturers are increasing the number of electric models [1,2], lithium-ion battery manufacturers are steadily increasing the investments in R&D [3], and the cities are adopting successful measures to motivate users to adopt EVs [4-6]. These incentives, among environmental consciousness and the drastic decrease in the operating costs (€/km) [7], have lead many users to adopt the use of EVs.

However, EVs also face huge challenges: first, the battery cost, which is about one-third of the EV cost [7]; secondly, the battery degradation and its lifetime; and thirdly, the charging time, which is moderately long. In this paper, we will address the last two aspects.

Currently, a standard charge on commercial midrange EVs (160 km) takes from six to eight hours [8,9]. This charging time is impractical in some situations. According to the U.S. Advanced Battery Consortium (USABC), the long term goal for fast charging is to return 40-80% of the battery state of charge (SOC) within 15 min [10]. Therefore, fast charging is a desirable functionality and consequently, an important subject to study.

The problem is that fast charging typically involves high current rates, high energy throughputs and high temperatures, all of which force the deterioration of battery's electric characteristics [11,12]. Then, the goal is to charge quickly with the minimal degradation effects. Regarding this topic, several works have been published from the era of Lead-Acid [13] to Nickel-Metal Hydride [14] and, more recently, Lithium-Ion [15,16].

However, it is necessary to improve the characteristics of fast charging techniques. In this way, we recently developed a fast charging technique on LFP batteries that meets the fast-charge USABC goals in terms of charging time, energy efficiency and cycle life [17]. This technique is experimental and it has not been yet implemented in EV´s, but their principles can be easily applied in real situations: a multistage charging process with high energy efficiency and minimum battery temperature rising [17].

The objective of this work is to analyse how different situations affect the battery functionality during long term testing: fast charge, high rate discharges and dynamic stressful tests (DST) at different depth of discharge (DOD). The battery performance is evaluated versus USABC targets [10] such as cycle life, fast charging, specific power (W/kg), specific energy (Wh/kg) and energy efficiency.

In this work, four LFP batteries from A123 manufacturer were tested at ambient temperature (23 ºC), completing previous studies [19]. Although nowadays many battery technologies are used in EVs [2,3], LFP batteries have key advantages, including: safety, high power capability, good cycle-life, fast charge ability and low cost [18].

The results provide useful information for its potential use in EVs, Battery Management System (BMS), among other applications as battery modelling. Furthermore, the test results are being used in actual studies on cell degradation mechanisms [20].

2 Experimental

In this study, a group of four nanophosphate A123 Systems ANR26650 commercial cells were tested. This type of batteries are presented by the manufacturer as a high power, versatile and long calendar life battery, suitable for portable high power devices, commercial trucks and hybrid electric vehicles (HEVs) [21]. Its main characteristics are summarized in Table 1.

The tests were carried out using a multichannel Arbin BT-2000 battery testing system. A Memmert environmental chamber was used to maintain a constant ambient temperature of 23ºC. The temperatures in both the climate chamber and the cell case were measured with T-type copper-constant thermocouples and logged into the Arbin system.

A123 Systems	ANR26650M1
Nominal cell capacity and nominal cell voltage	2.3Ah, 3.3V
Internal resistance (10A, 1s DC)	10 mΩ typical
Recommended standard charge method	3A to 3.6V CC/CV, 45min
Recommended fast-charge method	10A to 3.6V CC/CV, 15min
Cycle life at 10C discharge, 100% DOD	Over 1,000 cycles
Recommended charge and cut-off voltage at 25ºC	3.6V to 2V
Cell weight	70 grams

Table 1: ANR26650M1 battery characteristics from A123 manufacturer

2.1 Battery test procedures

The cells were subjected to the battery testing procedures shown in Fig. 1. The test starts with the commissioning, in which the batteries are identified and weighed. Next, the conditioning test sequence is performed according to the USABC constant current discharge series, described in [10]. During the conditioning, charge/discharge tests at C/25 are also performed; the measurements at this slow rate provide a practical capacity reference with minimal kinetic effects, which is close to the maximum capacity attainable by the cell [22].

The cycling procedure starts when the conditioning is finished. The cycling schedules perform a continuous charge and discharge test for 300 cycles. The cycling tests are particular for each of the tested cells (see Fig. 1.) and they are described in the following sub sections.

The reference test sequence includes various standard cycles and a final constant current charge/discharge cycle at C/25.

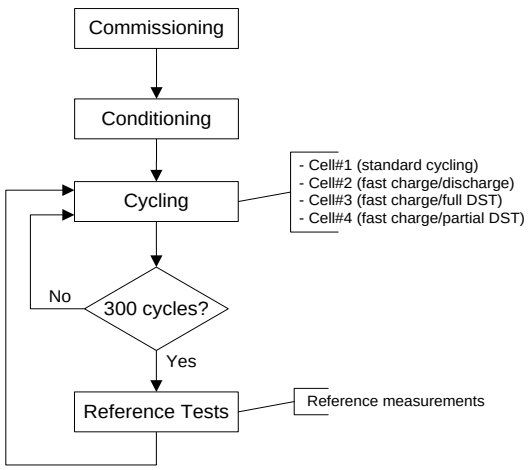

Fig. 1. Flow diagram of the testing procedure

This set of reference tests is mainly used to characterize the degradation during the cycle life of the test unit, and also to measure the cell's internal resistance. The resistance of the cell as a function of the rate C and the SOC can be calculated from Ohm's law (Eq. (1)) using the pseudo open circuit voltage (U pseudo – OCV) [22]:

$$R_{I1(C,\ SOC)} = \frac{U_{pseudo-OCV(SOC)} - U_{C(C,SOC)}}{|I1|} \quad (1)$$

In all the tests, the internal resistance is calculated at 50% SOC during both charging and discharging processes, from the voltage difference at 1 C rate.
After that the reference tests are finished, the cycling procedure is started again

2.2 Standard cycling test

The standard cycling test was carried out on Cell#1. This test consists of a continuous full charge and full discharge sequence at nominal conditions, as defined by the manufacturer. The charge is performed at 1 C constant current (CC) until the cell reaches the maximum charging voltage (3.6 V), followed by a constant voltage (CV) stage until the current declines to C/20. The discharge is performed at 1 C constant current until the cell reaches the cut off voltage (2 V). This sequence is repeated for 300 cycles, followed by the reference tests. Then again, the cycling is repeated.

2.3 Fast charging cycling test

This sequence test was carried out on Cell#2, and it consists of a continuous sequence of fast charge and full CC discharge.
The multistage fast charging technique developed by the researchers [17] is shown in Fig. 2. It consists of three different charging stages: the first stage (CC-I) is a CC charge at 4C until the battery reaches the maximum charging voltage (3.6 V). At this moment, the second stage (CC-II) starts, consisting of a CC charge at 1 C until 3.6 V. The last stage (CV-I) is performed at CV of 3.6 V for a duration of 5 min.The brief notation used in this work for this charging profile is 4C-1C-CV.
This fast charging technique is used because it meets the USABC long term fast charging goals [10], charging more than 90% of the battery capacity in less than 15 min, without accelerating the deterioration of the battery.

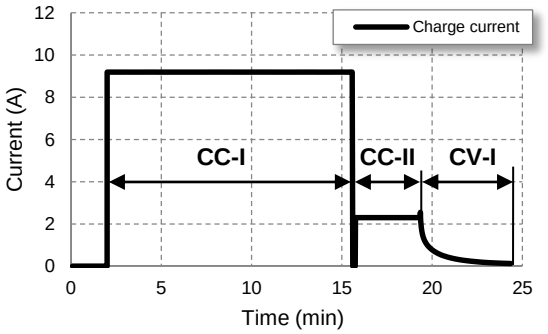

Fig. 2. Current profile for the fast charging technique

A complete analysis of fast charging technique applied can be found in reference [17].
The fast charging is followed by a CC discharge performed at 4 C, until battery voltage reaches the discharge cut off voltage (2 V). The discharge rate selected meets the long term USABC goal of specific power (400 W/kg).

2.4 Full dynamic stress cycling test

The full dynamic stress cycling test, performed on Cell#3, consists of the multistage fast charging technique (4C-1C-CV) previously described, and a dynamic stress test (DST) full discharge.
The discharge is carried out using a variable power discharge profile, developed by USABC [10]; the profile is shown in Fig. 3. The DST was scaled to the USABC long term goals, set to 400 W/kg. Moreover, the maximum power peak corresponds approximately to a 4 C discharge current for the tested cell.

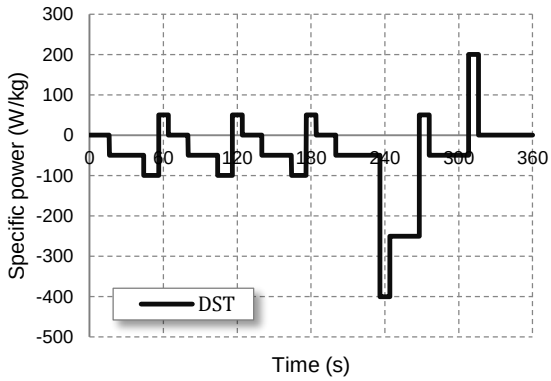

Fig. 3. Dynamic stress test protocol schedule

The full discharging sequence is finished when the voltage reaches the cut off voltage (2 V).
The profile of a complete fast charge and DST discharge cycle is shown if Fig. 4.

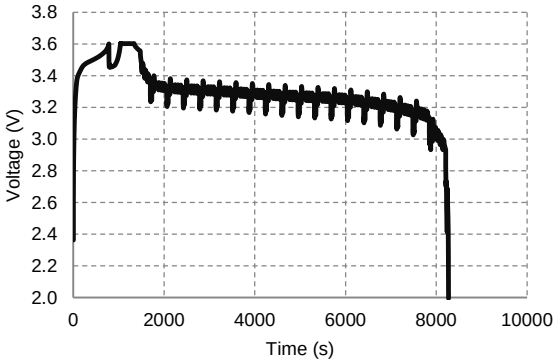

Fig. 4. Dynamic stress voltage profile for a complete charge and discharge cycle

2.5 Partial dynamic stress cycling test

The partial dynamic stress cycling test, performed on Cell#4, consists of the multistage fast charging technique (4C-1C-CV), and a partial dynamic stress test (DST) discharge. The partial discharge capacity is set to 1.15Ah, which is the half of battery nominal capacity. Fig. 5 shows two complete charge and discharge cycles of the tested protocol.

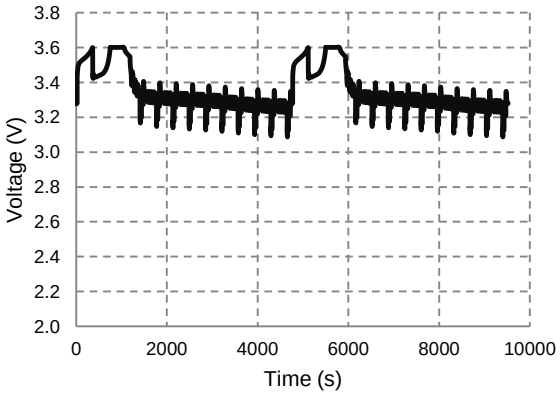

Fig. 5. Partial dynamic stress profile voltage for two complete charge and discharge cycles

3 Results

3.1 Conditioning results

To determine the effective capacity of the tested batteries, the conditioning tests were carried out. The nominal discharged capacity at 1 C adopted for this work is:

Cell#1 = 2.264 Ah
Cell#2 = 2.266 Ah
Cell#3 = 2.186 Ah
Cell#4 = 2.288 Ah

This indicates a capacity discrepancy of ≈5%. The results at C/25 show higher available capacity (≈2.5%) than at 1 C. Fig. 6 presents these results.

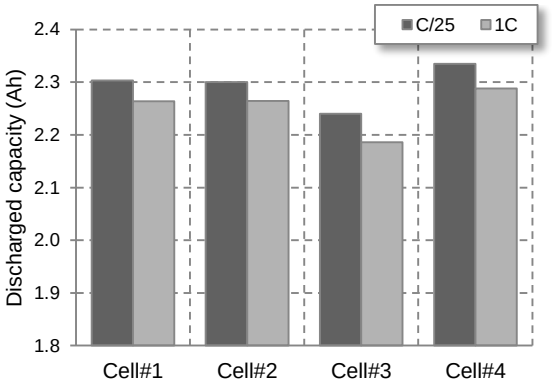

Fig. 6. Discharged capacities of the tested cells at conditioning tests

The batteries exhibit energy efficiencies in the range of 95% at 1 C and 99% at C/25, respectively. Based on the weight of the batteries, the results regarding to the specific energy for the discharge at 1 C are: 98.17 Wh/kg (Cell#1), 98.81 Wh/kg (Cell#2), 94.27 Wh/kg (Cell#3) and 104.4 Wh/kg (Cell#4). These values are below the minimum goals for long term commercialization, according to the USABC goals for advanced batteries for EVs [10].

Finally, the temperature in the batteries for the nominal tests is only 1 ºC above the ambient temperature (23 ºC).

3.2 Standard test (Cell#1)

The Cell#1 was tested for a total of 3000 cycles, which corresponded to a period of 13 months of continuous testing. As it can be seen in Fig. 7, the discharged capacity lost was over 10%, referred to the nominal capacity adopted (2.264 Ah). The capacity evolution follows a linear trend, and it is expected to reach its end-of-life at cycle ≈5000. End-of-life is defined by the USABC when a battery under a specific test protocol cannot deliver more than 80% of its nominal capacity, and the long term goal is set to 1000 cycles [10].

As it can be seen in Fig. 8, the energy efficiency during the whole testing procedure remains constant, with values of 99% for C/25 and 95% for 1 C. However, the discharged energy decreases linearly, following the same trend as the capacity decrease. Even if the battery reduces its performance in terms of discharged energy, its efficiency remains constant.

With regard to the internal resistance evolution with cycling, Fig. 9 shows a small increase of the internal resistance about 10% of the initial value.

Finally, as the battery was cycled under nominal conditions, its temperature was kept within the 24 ºC on average, with minimal variations.

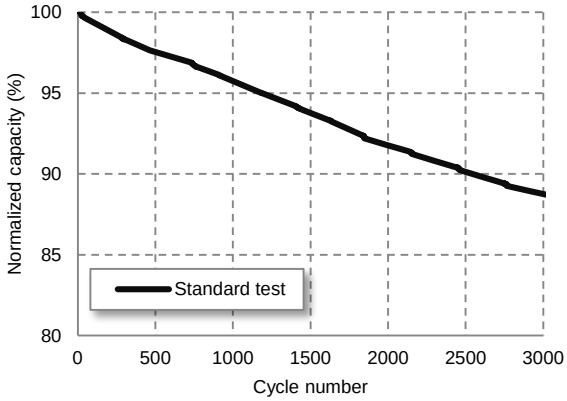

Fig. 7. Normalized discharged capacity evolution with cycling (Cell#1)

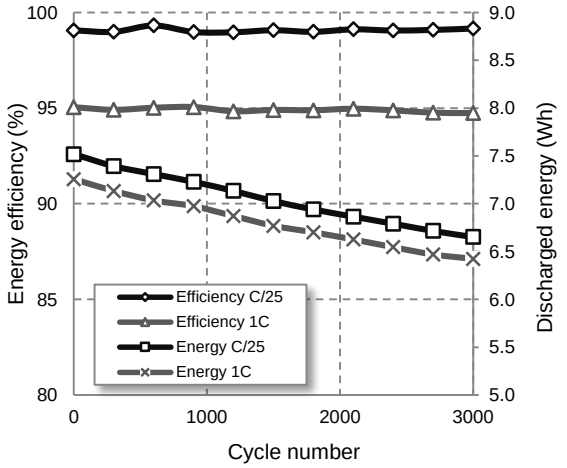

Fig. 8. Energy efficiency (left axis) and discharged energy (right axis) versus cycle number (Cell#1)

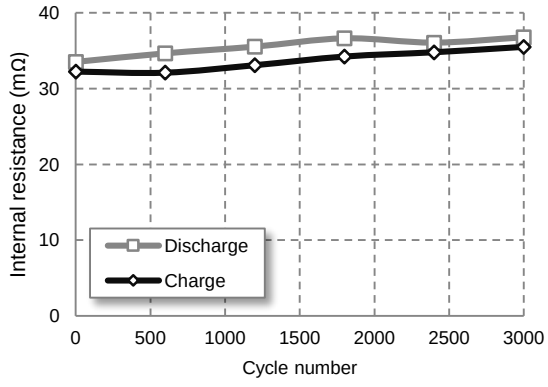

Fig. 9. Internal resistance vs. cycle number, both in charge and discharge (Cell#1)

3.3 Fast charge test (Cell#2)

This battery was tested using the fast charge technique (4C-1C-CV) and a full 4 C discharge for a period of 9 months, reaching a total of 4500 cycles.

During the testing, the battery experienced a capacity decrease of 17% of its nominal capacity (2.266 Ah). Fig. 10 shows the results during fast charge cycling, and also the results at C/25 obtained from the reference tests. Both curves show the same linear trend. The results obtained suggest that the battery will reach its end-of-life (80%) after approximately 5000 cycles. This number surpasses the USABC end-of-life goal regarding cycle life. The charging time during the whole cycling procedure was in the 25 min. range, charging up to 99% of the battery's total capacity.

Fig. 11 shows the battery temperature evolution through the experiment. The battery temperature never rose above 30 ºC and the average was about 27 ºC. The minimum temperatures reached at the end of the CV charging stage were slightly above the chamber temperature.

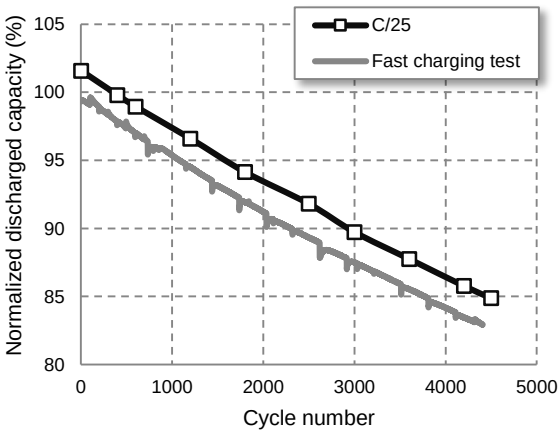

Fig. 10. Normalized discharged capacity evolution with cycling (Cell#2)

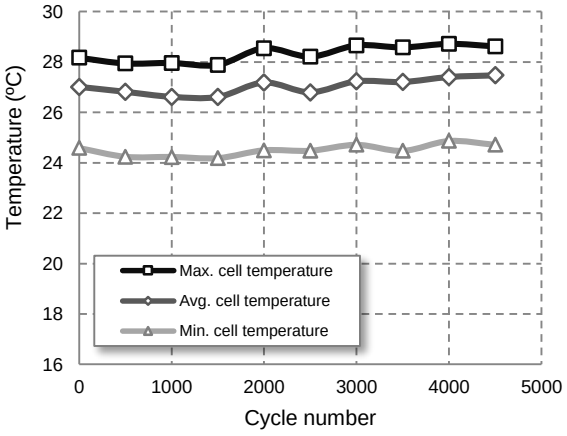

Fig. 11. Temperature evolution during cycling (Cell#2)

The internal resistance during cycling (see Fig. 12) fluctuated within the 5% margin, and there is no clear trend or increase in its values.

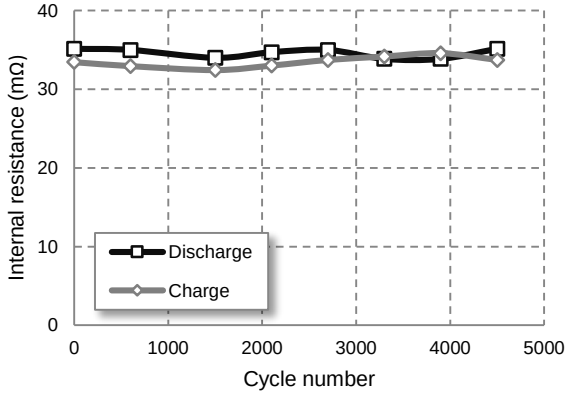

Fig. 12. Internal resistance vs. cycle number, both in charge and discharge (Cell#2)

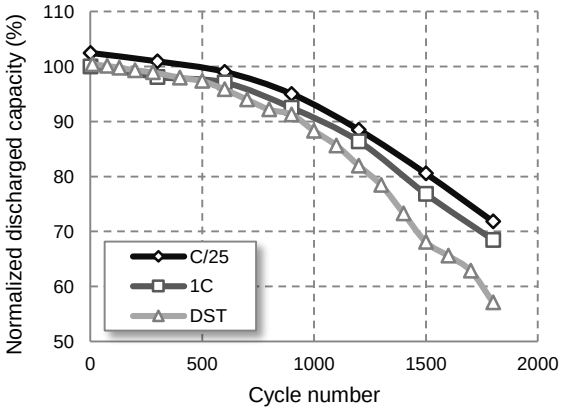

Fig. 13. Normalized discharged capacity evolution with cycling (Cell#3)

3.4 Full dynamic stress test (Cell#3)

Cell#3 was tested using the fast charge protocol (4C-1C-CV) and full DST discharges. The total number of cycles achieved in this experiment was 1800, and the testing time period lasted 8 months.

The fade of discharged capacity under DST is shown in Fig. 13, also under C/25 and 1 C reference tests. The tendency of the discharged capacity remains practically linear during the first 600 cycles. Then, the tendency changes and the capacity decreases more rapidly. At that point, it is also observed how the fast kinetics (DST) curve diverges from the thermodynamic C/25 and nominal 1 C tests. The end-of-life for this battery occurred at cycle 1200 for the DST cycling, and at cycle 1500 for the C/25 test.

The internal resistance evolution is shown in Fig. 14. The trend follows a constant increase until cycle 900, and then increases abruptly from the cycle 1200 to 1500. The total increase of the internal resistance during the complete test is about 40%.

The evolution of the charged capacity at the three different charging phases of fast charge technique (4C-1C-CV) is shown in Fig. 15. It is observed that at first, nearly all the cell capacity is charged under the first charging phase at 4 C. As the battery ages, the battery capacity decreases and the internal resistance increases; so, more capacity is charged during the 1 C phase. At cycle 1500, the capacity charged at 4 C and at 1 C phases is practically equal. The last phase at CV provides the final charge of battery.

With regard to the charging time, the duration of total charging process remains practically constant at 25 min. during cycling. However, the duration of both stages at 4 C and 1 C is modified.

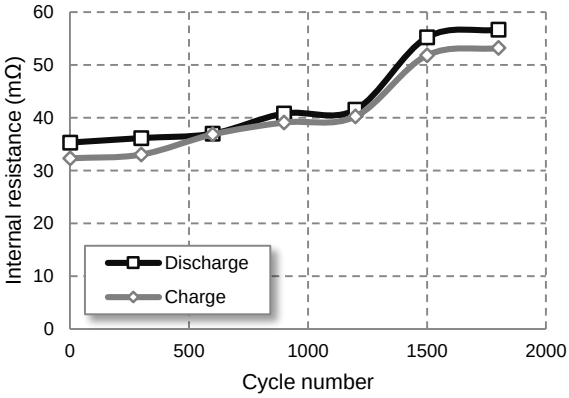

Fig. 14. Internal resistance vs. cycle number, both in charge and discharge (Cell#3)

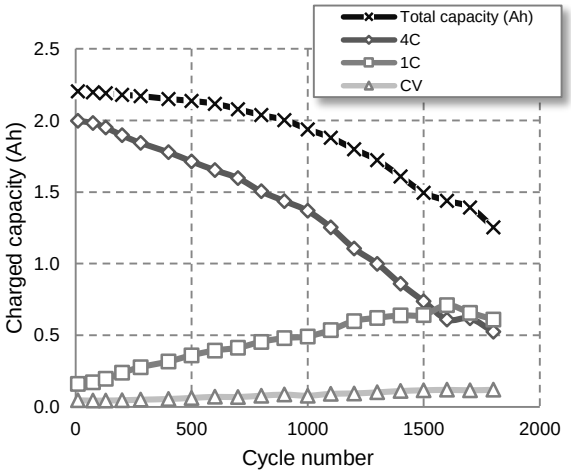

Fig. 15. Charged capacity evolution during the three different charging stages (Cell#3)

In this case, the two stages reached the same duration at cycle 700, about 10 min. The last phase at CV, with a fixed duration through cycling of 5 min. completes the charge procedure.

The battery temperature increasing during the testing procedure was within the 6 ºC range. The maximum temperature was 29 ºC, only reached for a moment at the end of the first charging stage at 4 C. During the DST discharges, since the average currents are low at approximately C/2, the temperature remains practically constant at 24 ºC. As a result, the average temperature of the battery during cycling remains practically constant in ≈24 ºC. The minimum temperatures are reached in the CV stage, at the end of charging process.

3.5 Partial dynamic stress test (Cell#4)

Cell#4 was tested using the fast charge technique (4C-1C-CV) and partial DST discharges, fixed to 50% of discharged capacity. The total number of cycles achieved in this experiment was 1200, and the testing time period was 4 months.

Fig. 16 shows the discharged capacity and the discharged energy, versus the cycle number. As the protocol was set to discharge 1.15 Ah, 50 % of the nominal battery capacity, the tendency is a constant line, as expected. The same trend is found with the discharged energy. However, this tendency would have decreased if the internal resistance had experienced an abrupt increase. We may have to go through a few more thousand cycles to see this effect emerge.

Reference tests are used to evaluate the capacity degradation of the battery with cycling. The evolution remains linear for all three tests. As it can be seen in Fig. 17, the end-of-life at 1 C is predicted at cycle ≈3000.

The internal resistance evolution in Cell#4 is shown in Fig. 18. The trend, both in charge and discharge remains practically constant, after a small increase of about 7% in the first 600 cycles.

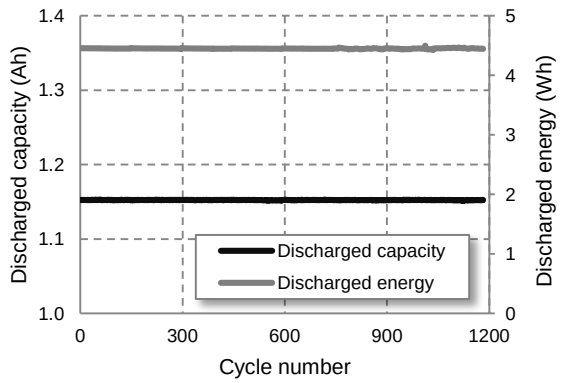

Fig. 16. Discharged capacity (left axis) and discharged energy evolution (right axis) with cycling (Cell#4)

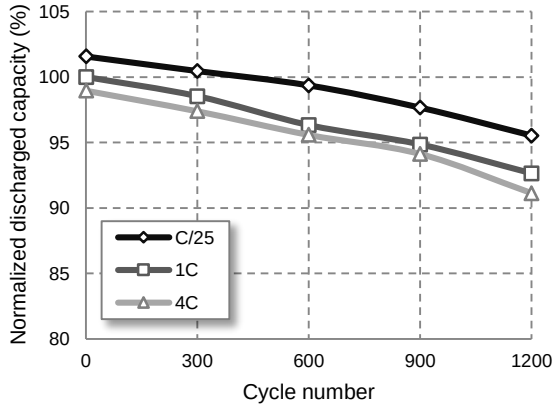

Fig. 17. Normalized discharged capacity evolution with cycling (Cell#4)

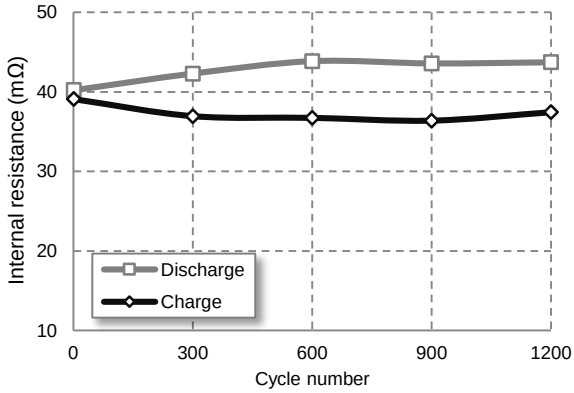

Fig. 18. Internal resistance vs. cycle number, both in charge and discharge (Cell#4)

The temperature variation for this testing is the same as with the previous full DST: maximum value (29 ºC) is reached at the end of the 4 C phase, and the average temperature for the whole process remains in the ≈24 ºC range.

4 Discussion

A set of four LFP batteries were extensively tested in this work. Cell#1 was cycled up to 3000 cycles at nominal rate, and it is used as a reference battery to establish comparative results with the other three batteries. Cell#2 to Cell#4 shared the same fast charge protocol, but the discharges were carried out at high constant current (4 C), full and partial DST protocols respectively.

From the results of this work, the battery end-of-life in each case is estimated. Both Cell#1 and Cell#2 follow the same linear trend in the evolution of fade capacity, and the prediction is that both will reach their end-of-life at cycle ≈5000. On the other hand, Cell#3 reaches its end-of-life at cycle 1200, whereas Cell#4 is predicted to reach it at cycle ≈3000.

Therefore, the cycle life of all tested cells meets the long term USABC goal regarding battery life, set to 1000 cycles.

It is understood that high rate cycling causes more rapid capacity fade [12]. However, this effect is not observed in this work when the same high rate is applied in charging and discharging processes: Cell#2 is cycled at stressful rates, four times higher than Cell#1, and the performance of both batteries is very similar. This effect could be related to the benefits of using a multistage fast charging protocol [13, 15, 17], but also to the battery's nanoparticles technology. Some studies suggest that this technology performs better at higher currents than lower ones [23].

On the other hand, the results obtained from both Cell#3 and Cell#4 confirm that the discharge dynamic stress tests strongly affect the battery life. On full DST discharges, the ageing processes are not linear; they follow a polynomial trend. This effect is also observed in other published works, under similar DST discharge procedures on li-ion batteries [24]. In addition, full DST discharges are more harmful than partial DST discharges. Also stated by Uwe [2] and others, the achievable capacity strongly depends on the depth-of-discharge, and the number of charge/discharge cycles increases exponentially with the reduction of the DOD. This is visible in our results, when comparing Cell#3 with Cell#4: full DST discharges reduces the battery life in a factor higher of 2.

External battery temperature measurements do not suggest any direct relationship with the battery degradation. The highest average temperature was ≈27 ºC for Cell#2, whereas for Cell#3 and Cell#4 was ≈24 ºC. High battery temperatures result in a significant battery degradation [11,12], but the values measured in these tests were not elevated (29 ºC was the highest temperature reached).

The internal resistance evolution with cycling was also calculated for all the tested batteries. Internal resistance is a key parameter, because it is directly linked to the power performance and the aging mechanisms of a battery, such as the solid electrolyte interface (SEI) growth or the physical degradation of the electrolyte structure [11,12]. The results show that when a battery is rapidly aged and the capacity evolution does not follow a linear trend (Cell#3), the internal resistance increases abruptly. However, if the capacity fade remains linear, the internal resistance does not increase unexpectedly, with changes within the 10%.

Cell#	Specific Energy (Wh/kg)	Specific Power (W/kg)	Cycle Life (cycles)	Fast-Charge (min)	Efficiency
USABC goals	80*	400	1,000	<15	80%
Cell#1	98	-	≈5000	-	95%
Cell#2	98	400	≈5000	<15	88%
Cell#3	94	400	1200	<15	91%
Cell#4	104	400	≈3000	<15	92%

*Mid-term goal

Table 2: USABC long-term goals achieved during the testing protocols

Moreover, the results show that when an optimum fast charging technique is applied, the fast charging is possible during long testing periods, without accelerating the deterioration of the battery (Cell#2). Multistage charging is a useful approach to fulfill fast charging objectives: short charging time, extended cycle life and efficient energy transfer. However, it is crucial the choice of the battery technology: high power LFP battery technology proves to be a choice. Experiments with fast-charging on hybrid buses with LFP demonstrate that 100% all electric operation is achievable [25]. Other battery technologies based on titanate, also have proved the ability of fast charging [16].

Therefore, several long term USABC goals were achieved in this work, summarized in Table 2. Fast charging is accomplished using the proposed fast charging protocol; specific energy, cycle life and energy efficiency are also met. However, the long term specific energy goal is not meet. This is one of the main disadvantages of LFP batteries for its use in EVs: they are heavier than other technologies [7,12].

5 Conclusion

In this work, LFP high power 2.3 Ah batteries were extensively tested and evaluated under standard, fast charge and DST cycling. In general, the tested batteries exhibited an overall good performance, throughout the battery cycle life.

The results show that an optimum fast charging technique can be performed successfully during the battery cycle life. The batteries tested at nominal 1 C rate and high 4 C rate are predicted to reach its end of life at 5000 cycles.

However, full DST discharges rapidly age the battery; in comparison to full CC discharges, only 1200 cycles have been reached.

In all tests developed, the long term USABC goals are achieved, including fast charging, cycle life and specific energy. However, long term specific energy goal is not meet, which is a drawback intrinsic in this technology.
Therefore, the results showed in this work provide useful information for the EV industry, as they could be taken into consideration for battery technology selection, BMS designs and other applications.
Follow up studies are being focused on the battery degradation mechanisms, to diagnose and prognosis how the battery aged.

Acknowledgments

The authors would like to thank the Spanish Ministry of Science and Innovation (MICINN) who provided the funding (TEC2009-12552) for this work.

References

[1] Wikipedia, *List of electric cars currently available*, www.wikipedia.org, accessed on 2013-06-25

[2] K. Uwe, *Lithium-Ion Batteries – Enabling Electric Mobility*, European Electric Vehicle Congress, 2012

[3] C. Pillot, *HEV, PHEV and EV market 2011-2025 - Battery is the key*, European Electric Vehicle Congress, 2012

[4] M. Molmen, *400 Public charging points in the city of Oslo 2008 – 2011*, European Electric Vehicle Congress, 2012

[5] R. Haaland, *Our future mobility: Oslo is the way to follow. Reasons and vision of a pioneer*, European Electric Vehicle Congress, 2012

[6] M. Linnenkamp, *Boosting electromobility*, European Electric Vehicle Congress, 2012

[7] S.F. Tie, C.W. Tan, *A review of energy sources and energy management system in electric vehicles*, Renewable and Sustainable Energy Reviews, ISSSN 1364-0321, 20 (2013), 82-102

[8] Renault Z.E., http://www.renault-ze.com/en-gb, accessed on 2013-06-25

[9] Mitsubishi i-MiEV, http://www.mitsubishi-cars.co.uk/imiev/, accessed on 2013-06-25

[10] United States Advanced Battery Consortium (USABC). *Electric Vehicle Battery Test Procedures Manual*, January 1996. http://www.uscar.org/guest/article_view.php?articles_id=86, accessed on 2013-06-25

[11] J. Vetter et. Al., *Ageing Mechanisms in Lithium-ion Batteries*, Journal Power Sources, ISSN 0378-7753, 147 (2005), 269-281

[12] W.J. Zhang, *Structure and performance of LiFePO4 cathode materials: A review*, Journal of Power Sources, ISSN 0378-7753, 196 (2011), 2962-2970

[13] T. Ikeya et. Al., *Multi-step constant-current charging method for electric vehicle, valve-regulated, lead/acid batteries during night time for load-levelling*, Journal of Power Sources, ISSN 0378-7753, 75 (1998), 101-107

[14] X.G. Yang and B.Y. Liaw, *Fast charging nickel-metal hydride traction batteries*, Journal of Power Sources, ISSN 0378-7753, 101 (2001), 158-166

[15] P.H.L. Notten et. Al., *Boostcharging Li-ion batteries: A challenging new charging concept*, Journal of Power Sources, ISSN 0378-7753, 145 (2005), 89-94

[16] A. Burke et. Al., *Fast charging tests (up to 6 C) of lithium titanate cells and modules: electrical and thermal response*, EVS26, Los Angeles, 2012

[17] D. Anseán et. Al., *Fast charging technique for high power lithium iron phosphate batteries: a cycle life analysis*, Journal Power Sources, ISSN 0378-7753, 239 (2013), 9-15

[18] B. Scrosati, and J. Garche, *Lithium batteries: Status, prospects and future*, J. Power Sources, ISSN 0378-7753, 195 (2010), 2419-2430

[19] D. Anseán et. Al., *Evaluation of LFP batteries using fast-charge and dynamic stress test protocols*, European Electric Vehicle Congress, 2012

[20] D. Anseán et. Al., *In preparation*

[21] A123 Systems, Inc, http://www.a123systems.com/products-cells-26650-cylindrical-cell.htm, accessed on 2013-06-25

[22] M. Dubarry and B.Y. Liaw, *Synthesize battery degradation modes via a diagnostic and prognostic model*, Journal of Power Sources, ISSN 0378-7753, 219 (2012), 204-216

[23] P. Bai, D.A. Cogswell, M.Z. Bazant, *Suppression of phase separation in $LiFePO_4$ nanoparticles during battery discharge*, Nano Letters, ISSN 1530-6984, 11 (2011) 4890-4896

[24] M. Dubarry and B.Y. Liaw, *Identify capacity fading mechanism in a commercial LiFePO4 cell*, Journal of Power Sources, ISSN 0378-7753, 194 (2009), 541-549

[25] R. Bedell, B. Westerlund, P. Åstrand, *First results from field testing of fast charged hybrid buses in Umeå, Sweden*, European Electric Vehicle Congress, 2011

Authors

David Anseán received the B.Sc. degree in Electronics Engineering from the University of Granada, Spain, in 2007. After gaining some industry experience in Basingstoke, UK, and Berkeley, CA, USA, in 2010 he joined the University of Oviedo, Spain, where he received the M.Sc. degree in Electrical Engineering in 2011, and where he is currently working towards his Ph.D. degree. His research interests include lithium ion batteries, particularly for its use in electric vehicles.

Juan Carlos Viera received the M.Sc. degree in Electrical Engineering from the University of Technology (ISPJAE), Havana, in 1992 and the Ph.D. degree in Electrical Engineering from the University of Oviedo, Spain, in 2003. He is currently an Assistant Professor in the Department of Electrical and Electronic Engineering, at the University of Oviedo, Spain. His research interests include battery management systems, battery testing, fast-charging among others.

Manuela González received the M.Sc. and the Ph.D. degrees in Electrical Engineering from the University of Oviedo, Spain, in 1992 and 1998, respectively. She is the founder and head of the Battery Research Laboratory in the Department of Electrical and Electronic Engineering, at University of Oviedo. Her research interests include battery management systems for new battery technologies and fast chargers for traction applications.

Víctor Manuel García is Professor in the area of Physical Chemistry at the University of Oviedo, Spain, with a doctorate in Quantum Chemistry and expertise in Theory of Electronic Separability. For several years his research interest has been focused on applied aspects of electrochemistry, either in batteries or corrosion. His research is coupled with an intense dedication to chemical education.

Juan Carlos Álvarez (M'08) was born in Veracruz, México, in 1966. He received the M.Sc. degree in Computer Engineering from the University of Valladolid (Spain) in 1996. He got his Ph.D. degree in 2007 from the University of Oviedo (Spain). He is currently with the Department of Electrical Engineering, University of Oviedo, as an Associated Professor. His research interests include lighting, electronic instrumentation systems and battery modeling.

José Luis Antuña received the M.Sc. in Industrial Electronic Engineer from the University of Oviedo, Spain, in 2007. He had a working grant at HC energy company during 2008. He also worked as researcher recycling industrial waste at School of Mines in 2009 and 2010. He is currently working towards the Ph.D. degree and as a researcher at the Battery Research Laboratory at University of Oviedo.